International Immunopharmacology 66 (2019) 41–51

Contents lists available at ScienceDirect

International Immunopharmacology

journal homepage: www.elsevier.com/locate/intimp

Methyl helicterte ameliorates liver fibrosis by regulating miR-21-mediated ERK and TGF-β1/Smads pathways

Quanfang Huang[a], Xiaolin Zhang[b], Facheng Bai[b], Jinlan Nie[b], Shujuan Wen[b], Yuanyuan Wei[b], Jinbin Wei[b], Renbin Huang[b], Min He[b], Zhongpeng Lu[c], Xing Lin[b,*]

[a] The First Affiliated Hospital of Guangxi University of Chinese Medicine, Nanning 530023, China
[b] Guangxi Medical University, Nanning 530021, China
[c] Department of Biochemistry, University of Arkansas Medical School, 4301 W. Markham, Little Rock, AR 72205-7199, USA

ARTICLE INFO

Keywords:
Methyl Helicterte
Hepatic fibrosis
Hepatic stellate cells
MicroRNA-21 (miR-21)
ERK pathway
TGF-β1/Smads pathway

ABSTRACT

Methyl helicterate (MH) has been reported to have protective effects against CCl_4-induced hepatic injury and fibrosis in rats, but its protective mechanism, especially on hepatic stallete cells (HSCs), remains unclear. Recently, our pilot experiment showed that MH could inhibit miR-21 expression in HSC-T6 cells, suggesting that miR-21 may be one of the targets of MH to intervene liver fibrosis. To verify the hypothesis, the present study would focus on the regulatory effect of MH on the miR-21-mediated ERK and TGF-β1/Smads pathways. Briefly, rats were intraperitoneally injected with 0.5 ml porcine serum (PS) twice a week for 24 weeks to induce liver fibrosis, and meanwhile, the rats were treated with MH from weeks 16 to 24. In vitro experiment, miR-21 expression in HSC-T6 cells was up- or down-regulated using lentiviral transfection assay. Collagen accumulation, inflammatory cytokines, cell apoptosis, miR-21 expression, and activation of the ERK and TGF-β1/smad2/3 pathways were then assessed. The results showed that MH treatment markedly alleviated PS-induced liver injury, as evidenced by the attenuation of histopathological changes and the decrease in serum alanine and aspartate aminotransferases activity. MH significantly decreased the content of inflammatory cytokines and recruited the anti-oxidative defense system. Moreover, MH treatment significantly decreased miR-21 expression and inhibited the activation of the ERK and TGF-β1/smad2/3 pathways in liver tissues. In vitro experiments showed that MH strongly inhibited HSC-T6 cell activation and reduced collagen accumulation. Interestingly, miR-21 overexpression significantly promoted HSC-T6 cell proliferation, reduced HSC apoptosis, and increased collagenation, while these abnormal changes induced by miR-21overexpression were significantly reversed by MH treatment. Furthermore, miR-21 overexpression notably activated the ERK and TGF-β1/Smads pathways via repressing SPRY2 and Smad7 expression respectively, however, these effects were largely abolished by MH treatment. In conclusion, our study demonstrates that MH significantly alleviates PS-induced liver injury and fibrosis by inhibiting miR-21-mediated ERK and TGF-β1/Smads pathways.

1. Introduction

Liver fibrosis, characterized by excessive accumulation of extracellular matrix (ECM), is a wound-healing process in response to chronic liver injuries. Hepatic stellate cells (HSCs) are the main source of the ECM, and their activation is a pivotal event in hepatic fibrogenesis [1]. HSC activation and proliferation are generally controlled by many intracellular signaling pathways, such as the TGF-β1/Smads and ERK/MAPKs pathways. Transforming growth factor beta 1 (TGF-β1) is the most potent fibrogenic factor in HSC activation by activating its downstream Smads signaling pathway [2]. Once activated, TGF-β binds to the membrane receptor, which further phosphorylates Smad2 and Smad3. Phosphorylated Smad2 and Smad3 then form a heteromeric complex with Smad4, and the complex translocates into the nucleus and activates the transcription of profibrotic genes [3]. In addition, the ERK/MAPKs signaling pathway is involved in cell proliferation, differentiation and migration. The ERK signal pathway has been found to play an important role in hepatic fibrosis via regulating the ECM synthesis [4]. Therefore, inhibiting HSC activation and promoting its apoptosis by modulating the TGF-β1/Smads and ERK signaling pathways are a potential strategy for the treatment of liver fibrosis [5].

* Corresponding author.
E-mail address: gxLx60@163.com (X. Lin).

https://doi.org/10.1016/j.intimp.2018.11.006
Received 23 August 2018; Received in revised form 26 October 2018; Accepted 5 November 2018
Available online 09 November 2018

Table 1
Primer sequences used in this study.

Genes	Primer	Sequence (5′-3′)
miR-21	RT stem-loop	GTCGTATCCAGTGCAGGGTCCGAGGTATTCGCACTGGATACGACTCAACATC
	Forward	ATGGTTCGTGGGTAGCTTATCAGACTGA
	Reverse	GCAGGGTCCGAGGTATTC
α-SMA	Forward	AGAAGCCCAGCCAGTCGCCATCA
	Reverse	AGCAAAGCCCGCCTTACAGAGCC
Col-I	Forward	GACATGTTCAGCTTTGTGGACCTC
	Reverse	AGGGACCCTTAGGCCATTGTGTA
Col-III	Forward	TTTGGCACAGCAGTCCAATGTA
	Reverse	GACAGATCCCGAGTCGCAGA
CTGF	Forward	TCAACCTCAGACACTGGTTTCG
	Reverse	TAGAGCAGGTCTGTCTGCAAGC
Smad2	Forward	TTACAGATCCATCGAACTCGGAGA
	Reverse	CACTTAGGCACTCGGCAAACAC
Smad3	Forward	GCACAGCAAGTTCCCAGTGTGTA
	Reverse	TGACAACTGAAATGCTGATCCAAAG
SPRY2	Forward	ATCAGAGCCATCCGAAACAC
	Reverse	CCTTGTACTGCTCCGAGACC
ERK1	Forward	TCCAAGGGCTACACCAAATC
	Reverse	AGGTAGTTTCGGGCCTTCAT
GAPDH	Forward	ACCACAGTCCATGCCATCAC
	Reverse	TCCACCACCCTGTTGCTGTA

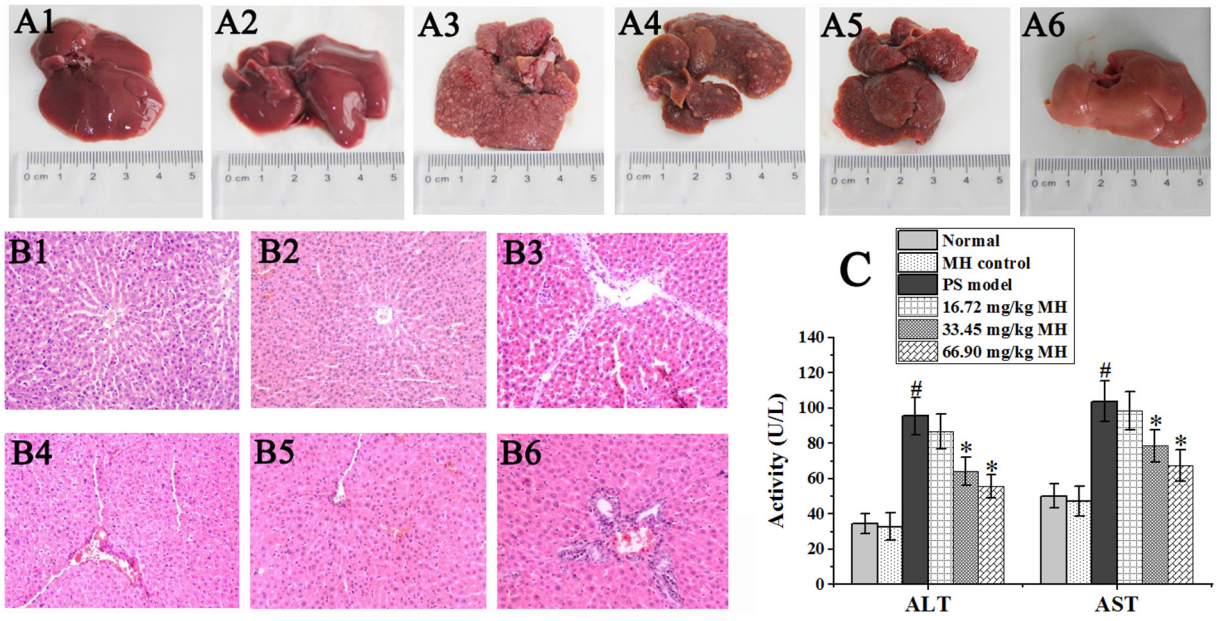

Fig. 1. MH ameliorated PS-induced liver injury. (A) The appearance of the liver samples. A1 to A6 represented the normal control group, MH control group, PS model group, 16.72, 33.45 and 66.90 mg/kg MH-treated groups, respectively. (B) The pathological change was observed by H&E staining (200 ×); B1 to B6 represented the normal control group, MH control group, PS model group, 16.72, 33.45 and 66.90 mg/kg MH-treated groups, respectively. (C) Serum ALT and AST activity was detected using commercial kits. $^{\#}P < 0.05$ VS. the normal control group and $^{*}P < 0.05$ VS. the model group.

MicroRNAs (miRNAs) are a class of endogenous, small (18–24 nucleotides) and non-coding single-stranded RNAs, which bind to the target genes and thereby repress translation of target genes and/or induce degradation of target gene mRNA. Dysregulation of miRNAs contributes to the development of a variety of diseases [6]. miRNA-21 is one of the most important microRNAs, which is a typical multi-functional miRNA to govern various signaling pathways, such as TGF-β1/Smads, ERK, PTEN/Akt and NF-κB signaling pathways. It has been reported that inhibiting miR-21 expression and subsequently blocking the TGF-β1/Smad7 and ERK1 signaling could attenuate hepatic fibrosis [7,8], suggesting that miR-21 may be served as a promising target for the treatment of hepatic fibrosis [9].

Many chemical compounds isolated from natural herbs have been shown to have hepatoprotective effects. *Helicteres angustifolia* (Sterculiaceae) is a traditional herbal medicine in oriental countries. It has been used in traditional Chinese medicine for the treatment of immune disorder and liver disease. In our previous studies, we have isolated an active ingredient from this herb and identified it as methyl helicterate (MH). We found that MH significantly alleviated CCl_4-induced hepatic injury and fibrosis in rats [10,11]. Moreover, MH notably ameliorated liver injury induced by hepatitis B virus [12]. Recently, our pilot experiment showed that MH significantly inhibited miR-21 expression in HSC-T6 cells, suggesting that MH ameliorated liver fibrosis maybe by regulating the potential target miR-21. However, it's not yet clear how MH regulates miR-21-mediated ERK and TGF-β1/Smads signaling pathways. Therefore, in the present study, the protective effect of MH against porcine serum (PS)-induced liver fibrosis in rats was evaluated and its underlying mechanism on regulating HSC activation was also investigated by targeting the miR-21-regulated ERK and TGF-β1/Smads signaling pathways.

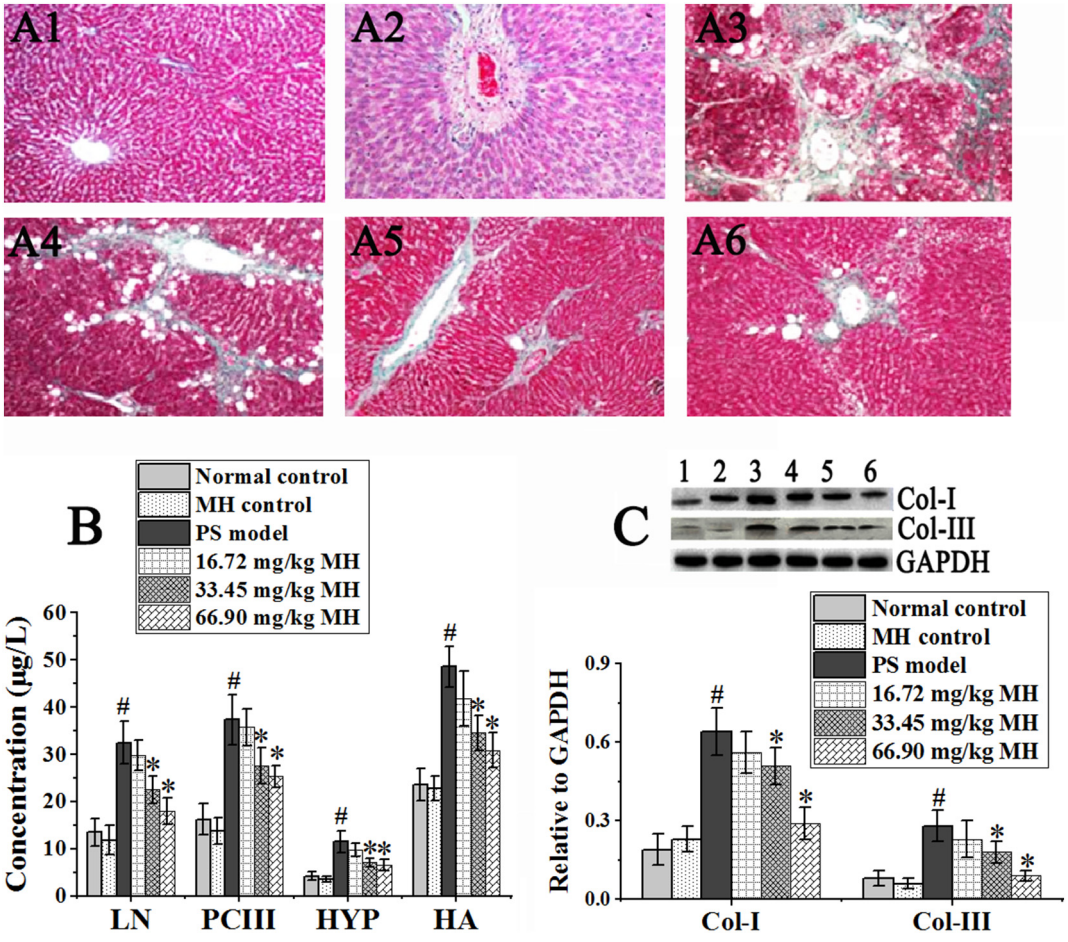

Fig. 2. MH alleviated PS-induced collagen accumulation. (A) The deposition of collagen was observed by Masson's trichrome staining (200 ×); A1 to A6 represented the normal control group, MH control group, PS model group, 16.72, 33.45 and 66.90 mg/kg MH-treated groups, respectively. (B) Serum HA, LN and PC III, and hepatic HYP were detected using commercial kits. (C) The protein expression of collagen I and III (Col-I and -III) was detected by Western blotting. Band 1 to 6 represented the normal control group, MH control group, PS model group, 16.72, 33.45 and 66.90 mg/kg MH-treated groups, respectively. $^{\#}P < 0.05$ VS. the normal control group and $^{*}P < 0.05$ VS. the model group.

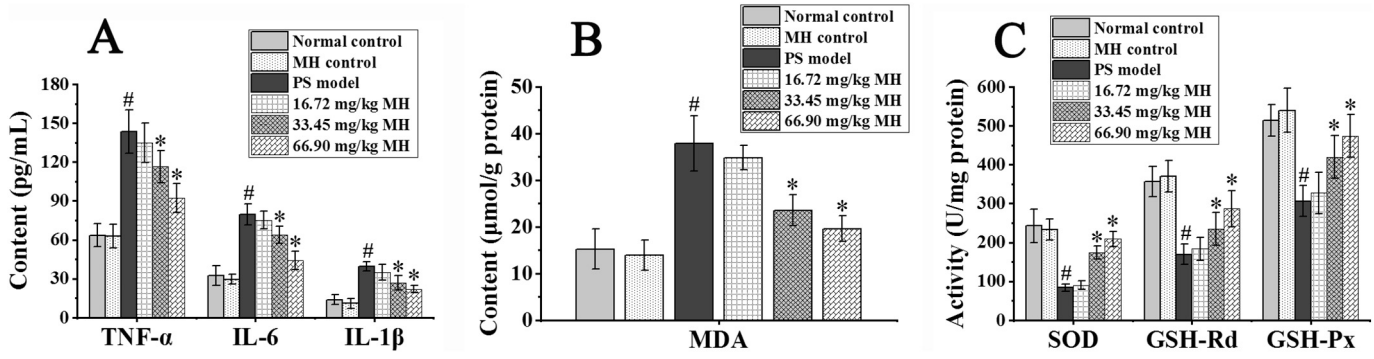

Fig. 3. MH alleviated PS-induced inflammatory response. (A) The inflammatory cytokines including serum TNF-α, IL-6 and IL-1β were detected using commercial kits. (B) MDA in liver tissue was detected using a thiobarbiturate method. (C) The activity of SOD, GSH-Px and GSH-Rd was detected using commercial kits. $^{\#}P < 0.05$ VS. the normal control group and $^{*}P < 0.05$ VS. the model group.

2. Materials and methods

2.1. Animals and treatments

Male Wistar rats (150 ± 10 g, SPF) were provided by the Experimental Animal Center of Guangxi Medical University (Guangxi, China) and were housed under controlled conditions with temperature of 25 ± 2 °C, relative humidity of 60 ± 10%, and a 12-h light/dark cycle. The animal experiment was approved by the Institutional Animal Care and Use Committee, Guangxi Medical University.

Hepatic fibrosis was induced by porcine serum (PS) as previously described [13] and the animal experiment was performed one time. Briefly, after acclimation for one week, rats were randomly divided into six groups (15 rats per group) including the normal control group, MH control group (66.90 mg/kg MH), model control group, and MH-treated groups (16.72, 33.45 and 66.90 mg/kg MH). The rats in the model

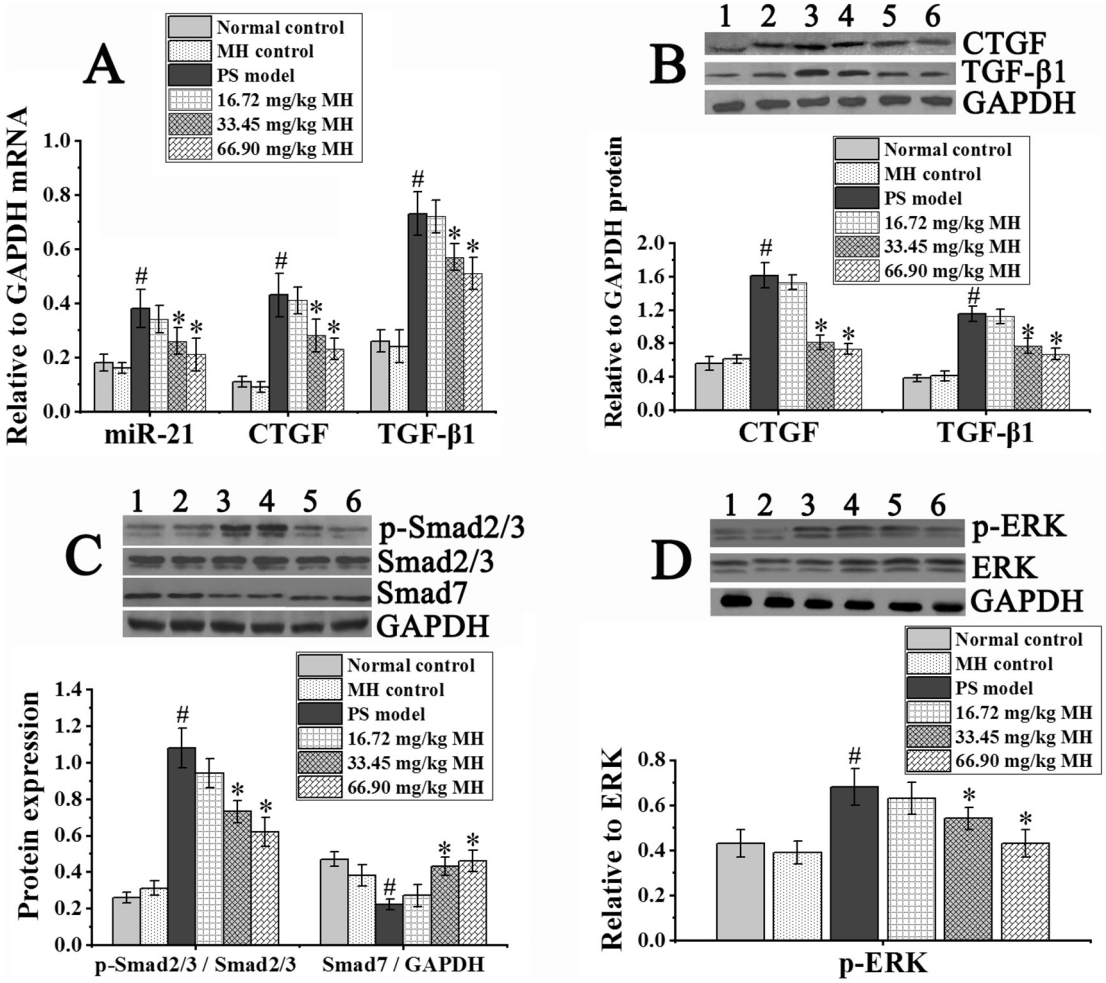

Fig. 4. MH inhibited miR-21 expression and thereby inhibited the TGF-β1/Smads and ERK pathways in PS-induced hepatic fibrosis. (A) The mRNA levels of miR-21, connective tissue growth factor (CTGF) and TGF-β1 were assessed using real-time PCR analysis. (B–D) The protein expression of CTGF, TGF-β1, Smad7, and the phosphorylation of p-Smad2/3 and p-ERK were detected by Western blotting; band 1 to 6 represented the normal control group, MH control group, PS model group, 16.72, 33.45 and 66.90 mg/kg MH-treated groups, respectively. $^{\#}P < 0.05$ VS. the normal control group and $^{*}P < 0.05$ VS. the model group.

control and MH-treated groups were intraperitoneally injected with 0.5 ml porcine serum (Beijing Solarbio Science & Technology Co., Ltd., Beijing, China) twice a week for 24 weeks to induce liver fibrosis; and the rats in the normal and MH control groups received an equivalent normal saline. Meanwhile, from weeks 16 to 24, the rats in the MH control and MH-treated groups were given intragastrically with various dosages of MH; and the rats in the normal and model control groups were given the same volume of saline. All animals were sacrificed at the end of treatment; and the blood and liver samples were obtained for further examination.

2.2. Pathological examination of liver tissues

Liver tissues were instantly removed and fixed with 10% phosphate buffered formalin, embedded in paraffin and sectioned into 5-μm slices, and then the samples were stained with hematoxylin and eosin (H&E) staining and Masson's trichrome staining as previously described [14] to evaluate the hepatic pathological change and fibrosis degree, respectively.

2.3. Serological test

Activity of alanine transaminase (ALT) and aspartate transaminase (AST) in serum was measured using commercially available kits (Nanjing Jiancheng Bioengineering Research Institute, Nanjing, China) and serum TNF-α, IL-6 and IL-1β were detected by sandwich enzyme-linked immunosorbent assay (ELISA) (Wuhan Boster Bio-engineering Co., Ltd., Wuhan, China) according to the protocol.

2.4. Assessment of antioxidant enzyme and lipid peroxidation

Liver homogenate was prepared as previously described [15]. The activity of superoxide dismutase (SOD), glutathione peroxidase (GSH-Px) and glutathione reductase (GSH-Rd) was determined using commercially available kit (Nanjing Jiancheng Bioengineering Institute, Nanjing, China) according to the manufacturer's instructions. Moreover, the extent of lipid peroxidation was estimated in liver homogenate by measuring the level of malondialdehyde (MDA) using a thiobarbiturate method [16].

2.5. Determination of the indicators of collagen

Serum hyaluronic acid (HA), type III precollagen (PCIII) and laminin (LN) were determined by radioimmunoassay (RIA) using commercially available kits (Beijing Furui Bioengineering Research Company, Beijing, China). Moreover, hepatic collagen was assessed by measuring hydroxyproline (HYP) content in fresh liver samples using commercially available kits (Nanjing Jiancheng Bioengineering Research Institute, Nanjing, China).

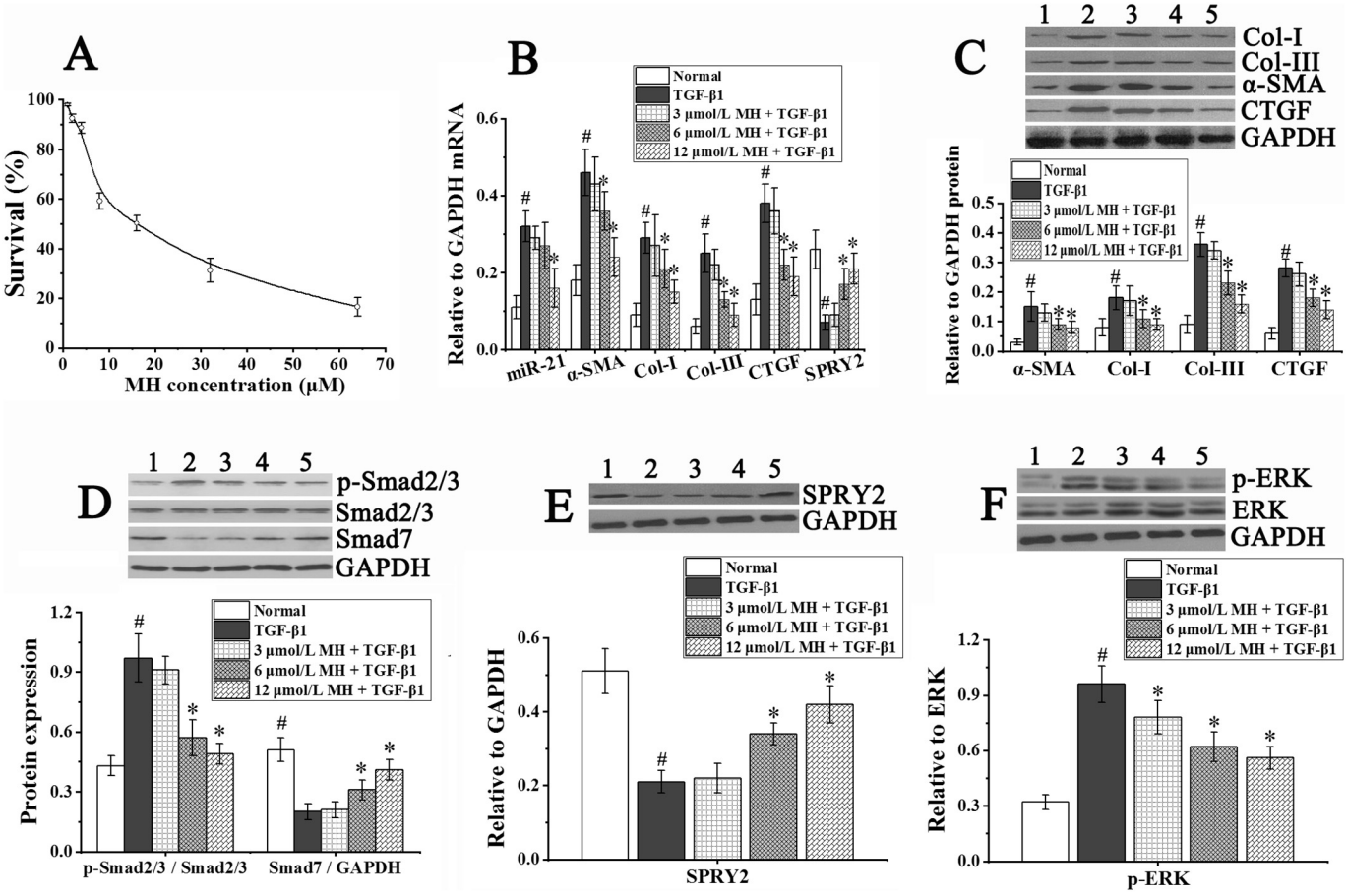

Fig. 5. Effects of MH on cell viability, miR-21 expression as well as the TGF-β1/Smads and ERK pathways after TGF-β1 stimulation in HSC-T6 cells. (A) Cytotoxicity of MH on HSC-T6 cells was assessed using MTT assay. (B) The mRNA levels of miR-21, α-SMA, Col-I, Col-III, CTGF and SPRY2 in HSC-T6 cells were assessed using real-time PCR analysis. (C) The protein expression of α-SMA, Col-I, Col-III, CTGF, Smad7, SPRY2 and the phosphorylation of p-Smad2/3 and p-ERK were detected by Western blotting; band 1 to 5 represented the normal control group, TGF-β1 group, 3, 6 and 12 μmol/l MH-treated groups, respectively. $^{\#}P < 0.05$ VS. the normal control group and $^{*}P < 0.05$ VS. the TGF-β1 group.

2.6. Cell culture and treatment

HSC-T6 cells were cultured with 1640 medium (1640, Hyclone) at 37 °C in a humidified air containing 5% CO_2 for 24 h. Then, cells were treated with various concentrations of MH (3.125, 6.25, 12.5, 25, 50 and 100 μmol/l) or equivalent DMSO (served as control) overnight and cytotoxic effect of MH on HSC-T6 cells was assessed using MTT assay as previously described [17].

Next, HSC-T6 cells were divided into five groups including the normal control group, TGF-β1 group (cells were treated with 10 ng/ml TGF-β1), and MH + TGF-β1 group (cells were treated with 10 ng/ml TGF-β1 plus 3, 6, or 12 μmol/l MH). Cells were plated in 6-well plates or 96-well plates for 24 h, followed by administration with the corresponding drugs for 24 h.

2.7. Knockdown or overexpression of miR-21 by lentivirus transfection

To inhibit miR-21 expression, a specific sequence for miR-21 (hsa-miR-21-3p inhibition: 5′-TCGAGAAAAAAACAGCCCATCGACTGGTGTTG TTTTTC-3′) and the reference sequence (5′-TTCTCCGAACGTGTCA CGT-3′) were synthesized as previously described [18]. GV369–miR-21/NC–enhanced green fluorescent protein (EGFP) was transfected into 293 T cells and the viral supernatant was harvested after 48 h (3×10^8 transducing units [TU]/ml). For overexpression, GV273–miR-21/NC–EGFP was transfected into 293 T cells and the supernatant was harvested after 48 h (3×10^8 TU/ml). HSC-T6 cells were plated in 6-well plates (3×10^5 cells per well) and incubated with the lentivirus at a multiplicity of infection (MOI) of ten according to the manufacturer's instructions (Genephama Biotech, Shanghai, China). The medium was replaced 12 h later, and the cells were grown for an additional time up to 72 h. Knockdown or overexpression of miR-21 was evaluated by real-time PCR analysis [18].

2.8. Determination of cell apoptosis

Cell apoptosis was evaluated by flow cytometry as previously described [19]. HSC-T6 cells were plated in 6-well plates (1×10^5 cells/well) overnight and then treated with drugs for 24 h. The treated cells were washed twice with PBS and harvested using centrifugation at 2000 rpm. After cells were resuspended with 500 μL of annexin, the Annexin-V-FITC Apoptosis Detection Kit (Bestbio, Shanghai China) was used to assess cell apoptosis according to the manufacturer's instruction.

2.9. Determination of caspase-3 and -9 activities

HSC-T6 cells were seeded in 6-well plates for 24 h and then treated with drugs overnight. Cells were washed with cold PBS twice, resuspended in lysis buffer and left on ice for 20 min. The lysate was centrifuged at 16,000 × *g* at 4 °C for 20 min. Supernatants were collected and protein concentrations were measured using the BCA™ Protein Assay Kit (Pierce, Rockford, IL, USA). Finally, caspase-3 and -9 activity was measured using commercially available kits (BioVision Research Products, Palo Alto, CA, USA) as previously described [20].

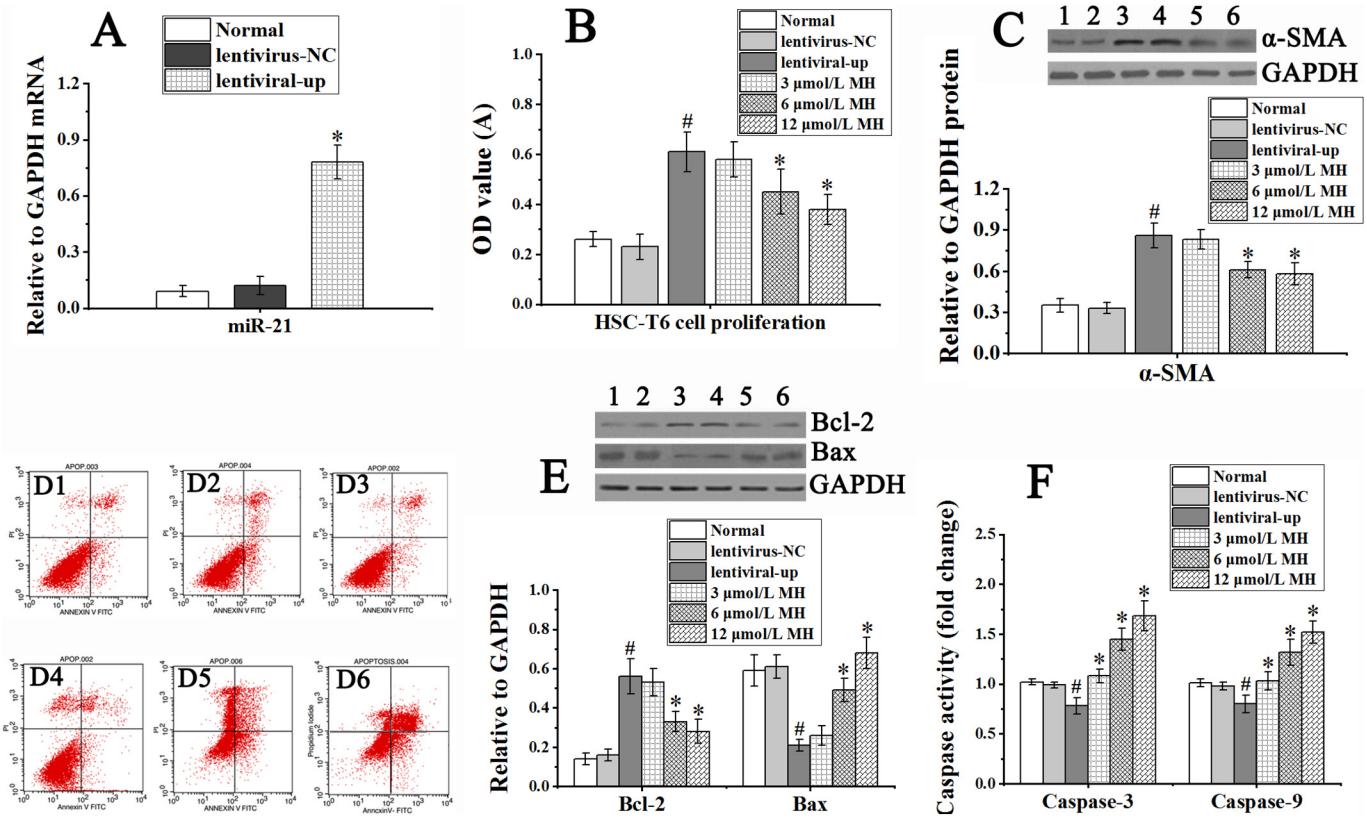

Fig. 6. MH significantly inhibited HSC-T6 cell activation and promoted cell apoptosis after miR-21 overexpression. (A) The mRNA level of miR-21 was detected by real-time PCR analysis. (B) HSC-T6 cell proliferation was assessed using MTT assay. (C and E) The protein expression of α-SMA, Bcl-2 and Bax was detected by Western blotting; band 1 to 6 represented the normal control group, lentivirus-NC group, lentivirus-up group, 3, 6 and 12 μmol/l MH-treated groups, respectively. (D) HSC-T6 cell apoptosis was detected by flow cytometry analysis; D1 to D6 represented the normal control group, lentivirus-NC group, lentivirus-up group, 3, 6 and 12 μmol/l MH-treated groups, respectively. (F) Caspase-3 and -9 activity was measured using commercially available kits. $^{\#}P < 0.05$ VS. the lentivirus-NC group and $^{*}P < 0.05$ VS. the lentivirus-up group.

Caspase activity was expressed as a ratio of the absorbance of control cells.

2.10. RT-PCR assay

Total RNA was extracted by TRIzol kit (KeyGEN BioTECH, Nanjing, China) according to the manufacturer's instructions. The RT-PCR assay was performed as previously described [20]. The primers used in this experiment were showed in Table 1.

2.11. Western blotting analysis

Western blotting was performed as previously described [21]. Briefly, total liver proteins were extracted from liver tissues using radioimmunoprecipitation buffer containing a protease inhibitor cocktail (Sigma-Aldrich); and whole cell proteins were prepared using RIPA buffer (Thermo Fischer Scientific, Inc., Waltham, MA) with 1% Halt protease inhibitor cocktail and 1% Halt phosphatase inhibitor cocktails (Thermo Fischer Scientific, Inc., Waltham, MA). The concentration of extracted protein was measured using BCA Protein Assay Kit (Beyotime, Jiangsu, China). The electrophoretic separation of the proteins was performed using 15% SDS-PAGE and electrotransferred to Immobilon-P membranes (Millipore, USA). The membranes were then incubated with primary antibodies overnight at 4 °C under agitation with the following primary antibodies: Col-I (1:500), Col-III (1:500), α-SMA (1:1000), CTGF (1:500), Bcl-2 (1:1000), Bax (1:1000), TGF-β1 (1:500), p-Smad2/3 (1:1000), Smad2/3 (1:1000), SPRY2 (1:500), ERK (1:500), p-ERK (1:500) and GAPDH (1:1000) (Santa Cruz Biotechnology). The membranes were washed three times using TBST for 5 min, and then incubated with horseradish peroxidase-labeled secondary antibody for 1 h. After three washes with TBST for 5 min each, protein bands were detected using an ECL Western blotting kit.

2.12. Statistical analysis

Statistical analysis was carried out using the Software of SPSS (Ver. 17.0). Different between groups were determined using a one-way ANOVA. The data are presented as means ± standard deviation (SD). $P < 0.05$ was considered to be statistically significant.

3. Results

3.1. MH ameliorated PS-induced liver damage

Administration of porcine serum (PS) causes a high incidence of hepatic fibrosis and, simultaneously, an immune response [22]. In the present study, we found that the livers in the normal and MH control groups were dark red in color, glossy in appearance and soft in texture (Panels A1 and A2). However, the samples in the PS model group showed a rough surface with numerous granules, firm texture, and pale red in color (Fig. 1A3). Interestingly, treatment with MH significantly ameliorated PS-induced pathological symptoms in a dose-dependent manner (Fig. 1A4 to A6). Moreover, the results of H&E staining showed that the hepatocytes in the normal control and MH control groups exhibited intact cellular architecture without necrosis, inflammatory infiltration or impaired progression (Fig. 1B1 and B2). In contrast, the rats in the PS model group showed intense chronic inflammatory infiltrate in portal areas with proliferation of biliary ducts; and scattered necrotic

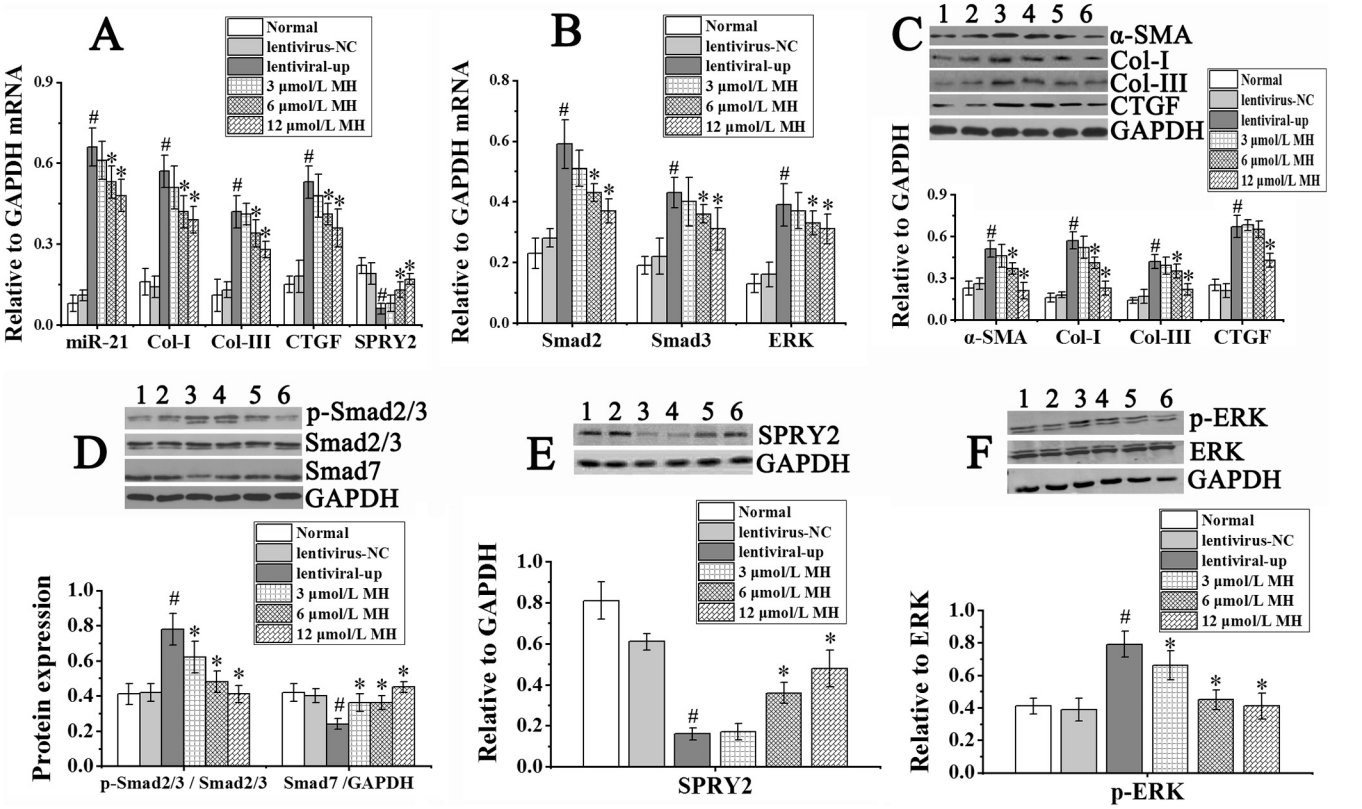

Fig. 7. MH significantly inhibited the TGF-β1/Smads and ERK pathways after miR-21 overexpression in HSC-T6 cells. (A and B) The mRNA levels of miR-21, Col-I, Col-III, CTGF, SPRY2, Smad2, Smad3 and ERK were detected by real-time PCR analysis. (C to F) The protein expression of α-SMA, Col-I, Col-III, CTGF, Smad7 and SPRY2, and the phosphorylation of p-Smad2/3 and p-ERK were detected by Western blotting; band 1 to 6 represented the normal control group, lentivirus-NC group, lentivirus-up group, 3, 6 and 12 μmol/l MH-treated groups, respectively. $^{\#}P < 0.05$ VS. the lentivirus-NC group and $^{*}P < 0.05$ VS. the lentivirus-up group.

and regenerative hepatocytes were also seen (Fig. 1B3). The animals treated with MH showed a striking reduction of inflammation and hepatocytes damage (Fig. 1B4 to B6). In addition, an analysis of serum ALT and AST activity was carried out to evaluate the degree of liver injury. As shown in Fig. 1C, the model group showed higher levels of ALT and AST than those of the normal control; however, both the enzymes were inhibited by MH treatment. Taken together, these results suggest that MH significantly ameliorates PS-induced liver injury.

3.2. MH alleviated collagen accumulation

The deposition and distribution of collage in liver tissue was observed by Masson's trichrome staining. The results revealed that the liver tissues from the normal control and MH control groups showed an intact lobular structure without obvious fibrosis accumulation (Fig. 2A1 and A2). However, administration with PS for 24 weeks caused extensive collagen deposition (Fig. 2A3). Treatment with MH significantly attenuated the degree of liver fibrogenesis, formation of pseudo-lobulus, and inflammatory cell infiltration (Fig. 2A4 to A6).

Next, the biomarkers of liver fibrogenesis, including HA, LN PC III and HYP, were further detected. The results showed that the content of these biomarkers was significantly increased in the PS model group. In contrast, the content of these biomarkers was decreased after treatment with MH (Fig. 2B). Moreover, PS administration led to an excessive protein expressions of collagen I and III (Col-I and -III); and it was not surprised that MH treatment reversed these abnormal changes in Col-I and -III induced by PS (Fig. 2C). These results suggest that MH significantly inhibits collagen accumulation, thereby alleviating hepatic fibrogenesis.

3.3. MH inhibited pro-inflammation cytokines and restored antioxidant enzymes

Inflammatory cytokines are the key trigger for the pathogenesis of liver injury. In this study, the content of TNF-α, IL-6 and IL-1β in the model group was higher than those in the normal control group. However, these up-regulations of inflammatory cytokines were markedly inhibited by MH treatment (Fig. 3A). In addition, excessive lipid peroxidation and decreased antioxidant enzyme activity are also associated with the pathological liver injury. As shown in Fig. 3B and C, administration of PS led to a significant increase in the activity of MDA (an end-product of lipid peroxidation) and a decrease in the activity of the antioxidant enzymes SOD, GSH-Px and GSH-Rd; however, MH treatment markedly reversed these abnormal changes induced by PS administration. These results suggest that MH treatment ameliorates PS-induced liver injury through inhibiting inflammatory response and restoring antioxidant enzymes, to some extent.

3.4. Effects of MH on miR-21 expression and the TGF-β1/Smads and ERK pathways in PS-induced hepatic fibrosis

The TGF-β1/Smads and ERK pathways play a vital role in the progress of liver fibrosis. Recent studies have shown that miR-21 can simultaneously regulate both of the signaling pathways. Thus, the effects of MH on miR-21 expression and the TGF-β1/Smads and ERK pathways in PS-induced hepatic fibrosis were evaluated in the present study. As shown in Fig. 4A, compared with the normal control group, the mRNA levels of miR-21, connective tissue growth factor (CTGF) and TGF-β1 in the model group were markedly increased. However, treatment with MH significantly decreased the mRNA levels of these genes compared with the model group. Moreover, as shown in Fig. 4B to D, compared

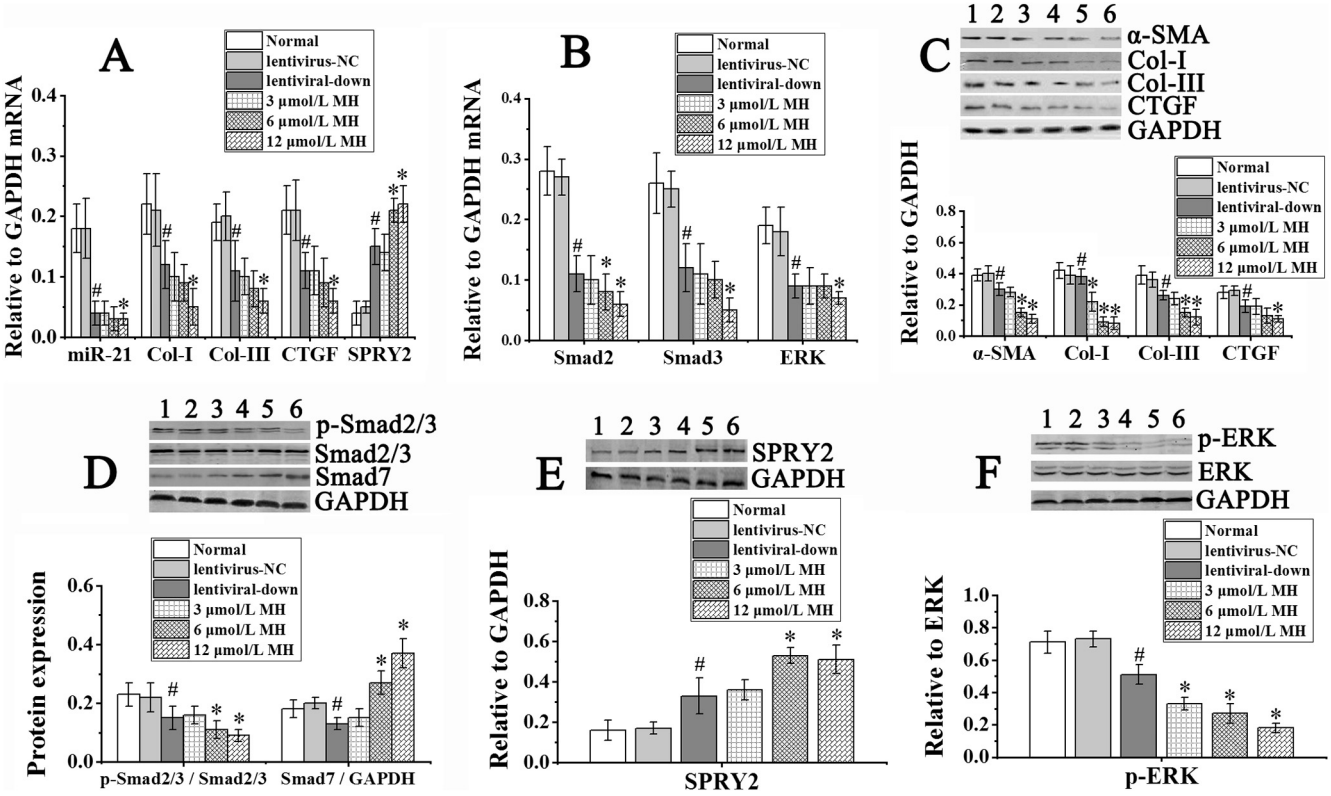

Fig. 8. MH inhibited the TGF-β1/Smads and ERK pathways after down-regulating miR-21 expression in HSC-T6 cells. (A and B) The mRNA levels of miR-21, Col-I, Col-III, CTGF, SPRY2, Smad2, Smad3 and ERK were detected by real-time PCR analysis. (C to F) The protein expression of α-SMA, Col-I, Col-III, CTGF, SPRY2 and Smad7, and the phosphorylation of p-Smad2/3 and p-ERK were detected by Western blotting; band 1 to 6 represented the normal control group, lentivirus-NC group, lentivirus-up group, 3, 6 and 12 μmol/l MH-treated groups, respectively. $^{\#}P < 0.05$ VS. the lentivirus-NC group and $^{*}P < 0.05$ VS. the lentivirus-up group.

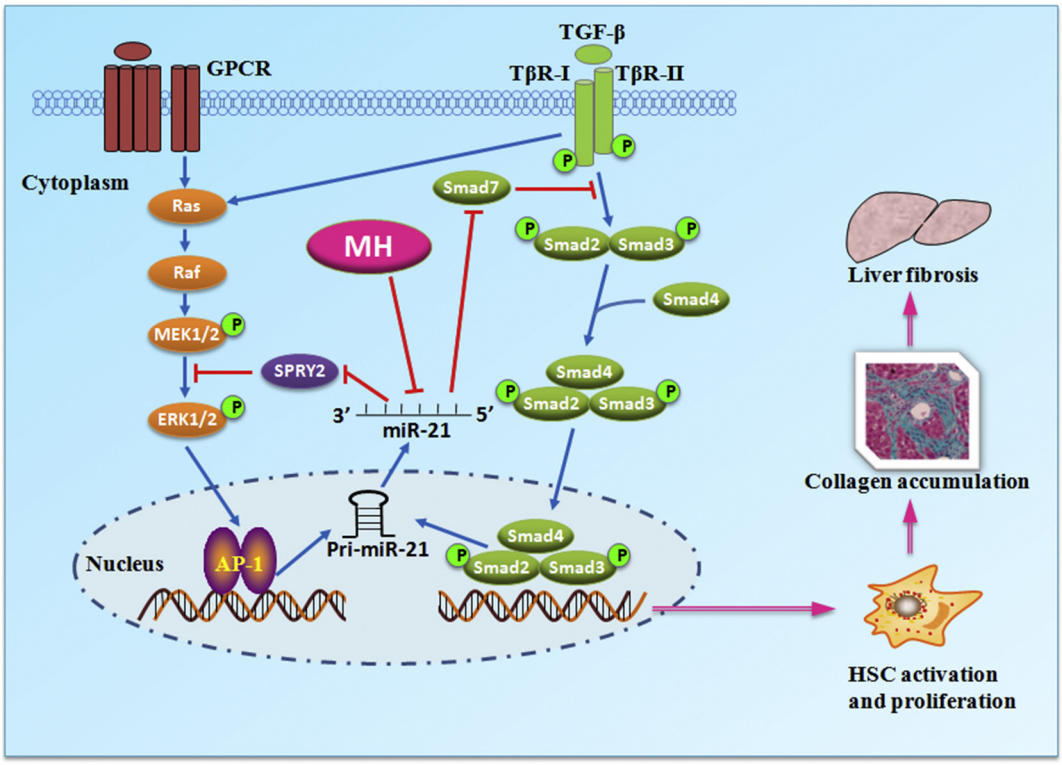

Fig. 9. MH ameliorates liver fibrosis by regulating miR-21-mediated ERK and TGF-β1/Smads pathways. Generally, miR-21 overexpression reduces the expression of SPRY2 and Smad7 and thereby relieves their inhibitory effects on the ERK and TGF-β1/Smads pathways, resulting in the activation of both the signaling pathways. MH can inhibit miR-21 expression and therefore block both the signaling pathways, inhibiting HSC activation and ultimately ameliorating liver fibrosis.

with the normal control group, the protein expression of CTGF and TGF-β1, and the phosphorylations of p-Smad2/3 and p-ERK were significantly increased, and the expression of Smad7 was markedly decreased. However, the abnormal expression of these proteins was significantly reversed by MH treatment. There data suggest that MH inhibits miR-21expression and subsequently blocks the TGF-β1/Smads and ERK pathways, ultimately inhibiting HSC activation and fibrogenesis.

3.5. Cytotoxicity of MH on HSC-T6 cells

Cytotoxicity of MH on HSC-T6 cells was assessed using MTT assay. As shown in Fig. 5A, MH significantly inhibited cell viability in a concentration-dependent manner and the 50% inhibitory concentration (IC50) was 12.73 μmol/l. Therefore, the concentration including 3, 6 and 12 μmol/l was chose for the further cell experiments.

3.6. Effects of MH on miR-21expression, HSC activation, collagenation and the TGF-β1/Smads and ERK pathways after TGF-β1 stimulation

The results showed that TGF-β1 stimulation led to a significant increase in the mRNA levels of miR-21, α-SMA, Col-I, Col-III and CTGF and a decrease in the level of SPRY2 in HSC-T6 cells compared with the normal control group. However, treatment with MH markedly reversed these genes expression in a concentration-dependent manner compared with the TGF-β1 group (Fig. 5B).

Moreover, western blot analysis showed that, compared with the normal control group, the protein expressions of α-SMA, Col-I, Col-III and CTGF and the phosphorylations of p-Smad2/3 and p-ERK in the TGF-β1-stimulated cells were significantly elevated, and the expressions of Smad7 and SPRY2 were significantly reduced. However, treatment with MH reversed the abnormal expressions of these proteins induced by TGF-β1 stimulation nearly to the normal levels (Fig. 5C to F). These results suggest that MH can reduce miR-21expression, HSC activation and collagenation, and inhibit the TGF-β1/Smads and ERK pathways in HSC-T6 cells.

3.7. Transduction efficiency of the miR-21 lentiviral vector GV369

In this study, the miR-21 lentiviral vector GV369 was constructed and then transfected into HSC-T6 cells. The green fluorescent protein (GFP) was observed using a fluorescence microscope (Olympus BX53; Olympus, Tokyo, Japan) after transfection for 72 h. To assess the transduction efficiency, the mRNA level of miR-21 was detected by real-time PCR. The results showed that there was no difference in the mRNA level of miR-21 between the normal control group and lentivirus-NC group (lentivirus negative control group). However, compared with the lentivirus-NC group, after transfection with miR-21 lentiviral vector GV369 (lentiviral-up group), the mRNA expression of miR-21 was significantly increased (nearly 8 times of the lentivirus-NC) (Fig. 6A). These results indicate that HSC-T6 cells transfected with miR-21 lentiviral vector GV369 exert overexpression of miR-21.

3.8. Effect of MH on HSC activation after miR-21 overexpression

HSC-T6 cells were plated in 6-well plates and transfected with the miR-21 lentiviral vector GV369 (lentiviral-up) for 72 h; and then cells were treated with MH at various concentrations (3, 6, or 12 μmol/l) for 24 h. The MTT assay showed that, compared with the miR-21 lentivirus-NC group, HSC-T6 cell proliferlation in the lentivirus-up group was significantly increased (Fig. 6B); moreover, the western blotting analysis showed that the protein expression of α-SMA was also significantly increased in the lentivirus-up group (Fig. 6C). Compared with the lentivirus-up group, MH treatment significantly inhibited HSC-T6 cell proliferation and α-SMA expression, suggesting that MH can inhibit HSC activation.

3.9. Effect of MH on HSC apoptosis after miR-21 overexpression

HSC-T6 cells were transfected with the miR-21 lentiviral vector GV369 and treated with MH as described above. Cell apoptosis was analyzed by Annexin V-FITC/PI staining using flow cytometry. The result showed that, compared with the lentivirus-NC group, miR-21 overexpression (lentiviral-up group) had little effect on HSC-T6 cell apoptosis (Fig. 6D). Moreover, miR-21 overexpression led to an increase in Bcl-2 protein expression, decrease in Bax level (Fig. 6E), as well as a decrease in the activity of caspase-3 and -9 (Fig. 6F). Interestingly, compared with the lentiviral-up group, MH treatment moderately increased cell apoptosis, decreased Bcl-2/Bax ratio, and enhanced the activity of caspase-3 and -9.

3.10. Effects of MH on miR-21-mediated TGF-β1/Smads and ERK pathways after miR-21 overexpression

HSC-T6 cells were transfected with the miR-21 lentiviral vector GV369 to induce miR-21 overexpression. We found that, compared with the lentivirus-NC group, the mRNA levels of miR-21, Col-I, Col-III, CTGF, Smad2, Smad3 and ERK were significantly increased and the mRNA level of SPRY2 was decreased in the lentivirus-up group; however, compared with the lentivirus-up group, the mRNA levels of the former seven genes were reduced and the mRNA level of SPRY2 was increased by MH treatment (Fig. 7A to B).

Similarly, compared with the lentivirus-NC group, the protein expressions of α-SMA, Col-I, Col-III and CTGF, as well as the phosphorylations of p-Smad2/3 and p-ERK were significantly increased (Fig. 7C to F), and the expressions of Smad7 and SPRY2 were decreased in the lentivirus-up group. Interestingly, compared with the lentivirus-up group, MH treatment significantly increased the expressions of Smad7 and SPRY2, but inhibited the expression levels of the other above proteins. These results demonstrated an inhibitory effect of MH on the miR-21-mediated TGF-β1/Smads and ERK pathways.

3.11. Transduction efficiency of the miR-21 lentiviral vector GV273

To down-regulate miR-21 expression, HSC-T6 cells were transfected with the miR-21 lentiviral vector GV273. The green fluorescent protein (GFP) was observed using a fluorescence microscope (Olympus BX53; Olympus, Tokyo, Japan) after transfection for 72 h. Compared with the lentivirus-NC group (lentivirus negative control group), HSC-T6 cells transfected with the miR-21 lentiviral vector GV273 (lentiviral-down) showed a significant decrease in the mRNA level of miR-21 (Fig. 8A), suggesting that miR-21expression was down-regulated.

3.12. Effects of MH on miR-21-mediated TGF-β1/Smads and ERK pathways after silencing of miR-21 expression

HSC-T6 cells were plated in 6-well plates and transfected with the miR-21 lentiviral vector GV273 (lentiviral-down) for 72 h, and then cells were treated with MH for 24 h. Compared with the lentivirus-NC group, the mRNA levels of miR-21, Col-I, Col-III, CTGF, Smad2, Smad3 and ERK in the lentivirus-down group were significantly decreased, and the mRNA level of SPRY2 was increased. After treatment with MH at a series of concentrations, the mRNA levels of miR-21, Col-I, Col-III, CTGF, Smad2, Smad3 and ERK were further decreased, and the SPRY2 level was further increased compared with the lentivirus-down group (Fig. 8A to B).

Moreover, as shown in the Fig. 8C to F, the protein expressions of α-SMA, Col-I, Col-III, CTGF, p-Smad2/3 and p-ERK in the lentivirus-down group were decreased, and the expressions of Smad7 and SPRY2 were increased. Treatment with MH further decreased the expressions of those former proteins and increased the expressions of Smad7 and SPRY2. These results further confirmed the inhibitory effect of MH on the miR-21-mediated TGF-β1/Smads and ERK pathways.

4. Discussion

Hepatic fibrosis can be induced by various pathogenic factors, such as viruses, alcohol, metabolic disorder and autoimmune disease. Most of the hepatic fibrosis models are so-called post-necrotic hepatic fibrosis; while porcine serum (PS)-induced rat hepatic fibrosis model is characterized by accompanying moderate hepatocyte damage. Changes in PS-induced hepatic fibrosis in rats have much similarity to the characters in human with hepatic fibrosis [23]. In this study, pathological examination showed that chronic PS administration caused a moderate damage to hepatic architecture and led to histological changes such as mononuclear cell infiltration, septum formation connecting portal tract with central veins; however, MH treatment significantly attenuated the degree of liver injury. Moreover, the serological assay revealed an increase in the activity of serum ALT and AST in the PS model group; while MH treatment notably decreased both the enzymes activity. Furthermore, our results showed that PS administration led to extensive accumulation of collagen; however, the increased collagen was significantly reduced by MH treatment. These results suggested that MH treatment significantly alleviates PS-induced hepatic injury and fibrosis in rats. Recently, our another study that investigated the underlying mechanism of MH on HSC apoptosis and autophagy once again confirmed that MH has strong protective effect against liver fibrosis in rats (data not shown).

Oxidative stress and consequent lipid peroxidation have been considered to be involved in liver fibrogenesis [24]. In order to clarify the mechanisms of hepatoprotective activity of MH, the content of the inflammatory cytokines (TNF-α, IL-6 and IL-1β), the level of lipid peroxidation (MDA) and the activity of the antioxidant enzymes (SOD, GSH-Px and GSH-Rd) were detected. Our results showed that MH treatment significantly decreased the contents of TNF-α, IL-6 and IL-1β and the level of MDA, but increased the activity of SOD, GSH-Px and GSH-Rd, suggesting that MH alleviates PS-induced liver injury partially by inhibiting oxidative stress and recruiting the anti-oxidative defense system.

HSCs are the major cellular source of intrahepatic ECM and play a key role in the process of hepatic fibrosis [25]. In this study, TGF-β1 stimulation significantly promoted HSC-T6 cell proliferation, increased the accumulation of collagen, and enhanced the expression of α-SMA; while MH treatment markedly reversed these abnormal changes induced by TGF-β1. These results demonstrated that MH has obvious inhibitory effect on the activation of HSCs, thereby reducing the accumulation of collagen.

In our previous studies, we found that MH has strong protective effects on the experimental liver injury and fibrosis induced by CCl_4, which largely may be associated with modulation of the TGF-β1/Smad3 pathway [10,11]. Recently, we found that MH treatment also significantly inhibited the MAPK/ERK pathway in HSC-T6 cells. However, the exact regulatory mechanism of MH on both the signaling pathways in HSCs remains unclear. Considering miR-21 is a key signaling molecule of the common upstream of both the signaling pathways, we predicted that the positive effect of MH on liver fibrosis may be achieved by regulating miR-21 expression level. miR-21 is a subtype of miRNAs family, which is a promising therapeutic target for liver fibrosis [8,26]. In the present study, the rats treated with PS or HSC-T6 cells stimulated with TGF-β1 showed a significant increase of miR-21 expression, but this uptrend was reduced by MH treatment, suggesting that MH can downregulate miR-21 expression in vivo and in vitro. Interestingly, overexpression of miR-21 significantly promoted HSC-T6 cell proliferation, reduced cell apoptosis, and led to collagen accumulation, indicating that overexpression of miR-21 is closely associated with the malignant progression of hepatic fibrosis. It was not surprise that these abnormal changes induced by miR-21 overexpression were significantly alleviated by MH treatment. Taken together, the above results demonstrated that miR-21 may be an important target for MH to intervene the process of hepatic fibrosis.

miR-21 plays a potential role in the pathogenesis of hepatic fibrosis via regulating some important signals, especially the ERK andTGF-β1/Smads signaling pathways. ERK signaling pathway is involved in cell growth, differentiation and migration of HSCs during liver fibrosis. Suppression of ERK1 signaling in HSCs could inhibit transformation of liver parenchymal and mesenchymal cells to activated fibroblasts, thereby attenuating hepatic fibrosis [27]. miR-21 could enhance the activity of ERK1 signaling by binding to the 3'-UTR of SPRY2, resulting in HSC activation [9]. In the present study, we found that up-regulating miR-21 expression in HSC-T6 cells led to a significant decrease in the expression of SPRY2 and an increase in the expression levels of α-SMA, Col-I, Col-III, CTGF and p-ERK; however, MH treatment largely abolished these abnormal changes induced by miR-21 overexpression. These results suggested that MH treatment inhibits miR-21 expression and thereby blocks the ERK signaling pathway.

miR-21 has also been shown to be participated in the TGF-β1 signaling pathway and aggravated the process of liver fibrosis [26]. Therefore, inhibiting miR-21 expression and thereby inhibiting the TGF-β1/Smad signaling pathway may be an effective strategy to ameliorate liver fibrosis. In vivo experiment of this study, the abnormal upregulations of miR-21, TGF-β1 and p-Smad2/3, as well as the downregulation of Smad7 in the PS-model group were obvious; while these abnormal expressions were markedly reversed by MH treatment. In vitro experiment, miR-21 overexpression led to an increase in the expression levels of α-SMA, Col-I, Col-III, CTGF, and p-Smad2/3, whereas caused a decrease in Smad7 expression level; and down-regulation of miR-21 expression led to opposite results. Interestingly, MH administration efficiently reversed these abnormal situations induced by miR-21 overexpression, suggesting that MH can inhibit the TGF-β1/Smads pathway via regulating miR-21 expression.

In conclusion, our study demonstrates that MH significantly ameliorates PS-induced liver fibrosis by inhibiting the miR-21-mediated ERK and TGF-β1/Smads pathways (Fig. 9), which will be developed as a potential medicine for the treatment of liver fibrosis. However, in order to more precisely illuminate the underlying mechanism of MH against hepatic fibrosis, further investigation is necessary to elucidate whether MH only selectively acts on hepatic stellate cells and whether it directly regulates miR-21expression.

Conflict of interest

The authors declare that there are no conflicts of interest.

Acknowledgments

The authors gratefully acknowledge the financial support provided by the National Natural Science Foundation of China (No. 81473431; No. 81660693; No. 81660686; No. 81660706), the Guangxi Natural Science Foundation (2016GXNSFDA380025), and Pharmaceutical Postgraduate Joint Cultivation Base for Innovation & Entrepreneurship (No. 20180606).

References

[1] M.J. Kim, S.A. Park, C.H. Kim, S.Y. Park, J.S. Kim, D.K. Kim, et al., TGF-β type I receptor kinase inhibitor EW-7197 suppresses cholestatic liver fibrosis by inhibiting HIF1alpha-induced epithelial mesenchymal transition, Cell. Physiol. Biochem. 38 (2016) 571–588.
[2] C. Liu, X. Chen, L. Yang, T. Kisseleva, D.A. Brenner, E. Seki, Transcriptional repression of the transforming growth factor β (TGF-β) pseudoreceptor BMP and activin membrane-bound inhibitor (BAMBI) by nuclear factor κB (NF-κB) p50 enhances TGF-β signaling in hepatic stellate cells, J. Biol. Chem. 289 (2014) 7082–7091.
[3] I. Fabregat, J. Moreno-Caceres, A. Sanchez, S. Dooley, B. Dewidar, G. Giannelli, et al., TGF-beta signalling and liver disease, FEBS J. 283 (2016) 2219–2232.
[4] F. Marra, W. Delogu, I. Petrai, S. Pastacaldi, A. Bonacchi, E. Efsen, et al., Differential requirement of members of the MAPK family for CCL2 expression by hepatic stellate cells, Am. J. Physiol. Gastrointest. Liver Physiol. 287 (2004) G18–G26.
[5] D. Schuppan, Y.O. Kim, Evolving therapies for liver fibrosis, J. Clin. Invest. 123

(2013) 1887–1901.
[6] I.M. Pedersen, G. Cheng, S. Wieland, S. Volinia, C.M. Croce, F.V. Chisari, et al., Interferon modulation of cellular microRNAs as an antiviral mechanism, Nature 449 (2007) 919–922.
[7] F. Yang, L. Luo, Z.D. Zhu, X. Zhou, Y. Wang, J. Xue, et al., Chlorogenic acid inhibits liver fibrosis by blocking the miR-21-regulated TGF-beta1/Smad7 signaling pathway in vitro and in vivo, Front. Pharmacol. 8 (2017) 1–13.
[8] K. Wu, C. Ye, L. Lin, Y. Chu, M. Ji, W. Dai, et al., Inhibiting miR-21 attenuates experimental hepatic fibrosis by suppressing both the ERK1 pathway in HSC and hepatocyte EMT, Clin. Sci. (Lond.) 130 (2016) 1469–1480.
[9] J. Zhao, N. Tang, K. Wu, W. Dai, C. Ye, J. Shi, et al., MiR-21 simultaneously regulates ERK1 signaling in HSC activation and hepatocyte EMT in hepatic fibrosis, PLoS One 9 (2014) e108005.
[10] Q. Huang, Y. Li, S. Zhang, R. Huang, L. Zheng, L. Wei, et al., Effect and mechanism of methyl helicterate isolated from *Helicteres angustifolia* (*Sterculiaceae*) on hepatic fibrosis induced by carbon tetrachloride in rats, J. Ethnopharmacol. 143 (2012) 889–895.
[11] X. Lin, R. Huang, S. Zhang, L. Zheng, L. Wei, M. He, et al., Methyl helicterate protects against CCl_4-induced liver injury in rats by inhibiting oxidative stress, NF-κB activation, Fas/FasL pathway and cytochrome P4502E1 level, Food Chem. Toxicol. 50 (2012) 3413–3420.
[12] Q. Huang, R. Huang, L. Wei, Y. Chen, S. Lv, C. Liang, et al., Antiviral activity of methyl helicterate isolated from *Helicteres angustifolia* (*Sterculiaceae*) against hepatitis B virus, Antivir. Res. 100 (2013) 373–381.
[13] F. Bai, Q. Huang, J. Wei, S. Lv, Y. Chen, C. Liang, et al., *Gypsophila elegans* isoorientin-2″-O-alpha-L-arabinopyranosyl ameliorates porcine serum-induced immune liver fibrosis by inhibiting NF-kappaB signaling pathway and suppressing HSC activation, Int. Immunopharmacol. 54 (2018) 60–67.
[14] Q. Huang, R. Huang, S. Zhang, J. Lin, L. Wei, M. He, et al., Protective effect of genistein isolated from *Hydrocotyle sibthorpioides* on hepatic injury and fibrosis induced by chronic alcohol in rats, Toxicol. Lett. 217 (2013) 102–110.
[15] Q.F. Huang, S.J. Zhang, L. Zheng, M. Liao, M. He, R. Huang, et al., Protective effect of isoorientin-2″-O-alpha-L-arabinopyranosyl isolated from *Gypsophila elegans* on alcohol induced hepatic fibrosis in rats, Food Chem. Toxicol. 50 (2012) 1992–2001.
[16] M.E. Shaker, H.A. Salem, G.E. Shiha, T.M. Ibrahim, Nilotinib counteracts thioacetamide-induced hepatic oxidative stress and attenuates liver fibrosis progression, Fundam. Clin. Pharmacol. 25 (2011) 248–257.
[17] Q. Huang, L. Wei, C. Liang, J. Nie, S. Lu, C. Lu, et al., Loss of Raf kinase inhibitor protein is associated with malignant progression in hepatic fibrosis, Biomed. Pharmacother. 82 (2016) 669–676.
[18] Y. Wang, F. Yang, J. Xue, X. Zhou, L. Luo, Q. Ma, et al., Antischistosomiasis liver fibrosis effects of chlorogenic acid through IL-13/miR-21/Smad7 signaling interactions in vivo and in vitro, Antimicrob. Agents Chemother. 61 (2017) 1–16.
[19] F. Bai, Q. Huang, J. Nie, S. Lu, C. Lu, X. Zhu, et al., Trolline ameliorates liver fibrosis by inhibiting the NF-κB pathway, promoting HSC apoptosis and suppressing autophagy, Cell. Physiol. Biochem. 44 (2017) 436–446.
[20] X. Lin, J. Wei, Y. Chen, P. He, J. Lin, S. Tan, et al., Isoorientin from *Gypsophila elegans* induces apoptosis in liver cancer cells via mitochondrial-mediated pathway, J. Ethnopharmacol. 187 (2016) 187–194.
[21] L. Xing, F. Bai, J. Nie, S. Lu, C. Lu, X. Zhu, et al., Didymin alleviates hepatic fibrosis through inhibiting ERK and PI3K/Akt pathways via regulation of Raf kinase inhibitor protein, Cell. Physiol. Biochem. 40 (2016) 1422–1432.
[22] E. Bhunchet, Y. Eishi, K. Wake, Contribution of immune response to the hepatic fibrosis induced by porcine serum, Hepatology 23 (1996) 811–817.
[23] Y. Baba, K. Saeki, T. Onodera, K. Doi, Serological and immunohistochemical studies on porcine-serum-induced hepatic fibrosis in rats, Exp. Mol. Pathol. 79 (2005) 229–235.
[24] M. Tamura, H. Matsui, T. Kaneko, I. Hyodo, Alcohol is an oxidative stressor for gastric epithelial cells: detection of superoxide in living cells, J. Clin. Biochem. Nutr. 53 (2013) 75–80.
[25] A.I. Serban, L. Stanca, O.I. Geicu, M.C. Munteanu, A. Dinischiotu, RAGE and TGF-β1 cross-talk regulate extracellular matrix turnover and cytokine synthesis in AGEs exposed fibroblast cells, PLoS One 11 (2016) e0152376.
[26] Z. Zhang, Z. Gao, W. Hu, S. Yin, C. Wang, Y. Zang, et al., 3,3′-Diindolylmethane ameliorates experimental hepatic fibrosis via inhibiting miR-21 expression, Br. J. Pharmacol. 170 (2013) 649–660.
[27] W. Zhong, W.F. Shen, B.F. Ning, P.F. Hu, Y. Lin, H.Y. Yue, et al., Inhibition of extracellular signal-regulated kinase 1 by adenovirus mediated small interfering RNA attenuates hepatic fibrosis in rats, Hepatology 50 (2009) 1524–1536.